

Analysis of the Thermal Deformation Behaviour of Ti₂AlNb-Based Alloys Based on a Modified and Optimised Zerilli-Armstrong Model

Jie LIU^a, Kelu WANG^{a,1}, Xin LI^a, Tong ZHOU^a and Zengqiang WANG^a

^a School of Aeronautical Manufacturing Engineering, Nanchang Hangkong University, Nanchang, 330063, China

Abstract. Isothermal constant strain rate compression of Ti₂AlNb-based alloys was carried out using a Gleeble-3500 thermal simulation tester with deformation temperatures of 650-850°C, strain rate interval of 0.001-1s⁻¹, on the basis of which a modified Zerilli-Armstrong model and an optimised Zerilli-Armstrong model were developed to describe the thermal deformation behaviour of Ti₂AlNb-based alloys. The results show that the error between the predicted and experimental values of the modified Zerilli-Armstrong model is larger, with correlation coefficients R and E_{AR} of 0.935 and 12.4% respectively, while the optimised Zerilli-Armstrong model can predict the flow stress better, with correlation coefficients R and E_{AR} of 0.964 and 10.5% respectively. The optimised Zerilli-Armstrong model had high prediction accuracy and wider applicability, making it more suitable as a constitutive model for predicting the thermal deformation behaviour of Ti₂AlNb-based alloys.

Keywords. Ti₂AlNb-based alloy, constitutive model, Zerilli-Armstrong model, flow stress

1. Introduction

Titanium alloys are widely used in aerospace, petrochemical and automotive fields, but their poor high-temperature performance is a drawback that limits their widespread use, while titanium-aluminum alloys, with their light weight and high-temperature oxidation resistance, are considered potential high-temperature structural materials for the aerospace industry [1-2]. And Ti₂AlNb-based alloys not only can inherit the advantages of traditional titanium alloy, but also is an advanced aerospace material with high specific strength, low density, good high-temperature oxidation resistance and creep resistance, which has attracted widespread attention and is an ideal lightweight high-temperature structural material for aero-engine weight reduction, and can be used to manufacture compressor discs, blades and other components [3-5].

In contrast, the Z-A model is a physical constitutive model [6-8] with small calculation, concise expressions, and higher accuracy than other physical instants,

¹ Kelu WANG, Corresponding author, Professor, School of Aeronautical Manufacturing Engineering, Nanchang Hangkong University, Nanchang, 330063, P.R. China; E-mail: wangkelu@126.com.

which can better account for the effects of strain rate, temperature, and strain on the flow stress. In recent years, some scholars have started to study various alloys using the Z-A model, and initial progress has been obtained [7,9]. Sim et al. [10] used the Z-A and Khan-Huang-Liang instantaneous models to predict the thermal deformation behavior of Ti-22Al-25Nb alloy at 950-1070°C and 0.001-1s⁻¹ and found that the optimized Z-A and KHL models were better predictors under the current study conditions and other deformation conditions, and the correlation coefficient of the Z-A model and the average relative error improved from 0.9773 and 8.73% before optimization to 0.9896 and 6.14%.

Currently, there is no report on the use of Z-A model to describe the thermal deformation behavior of Ti₂AlNb-based alloys. Therefore, the selection of a suitable constitutive model to predict the high-temperature deformation behavior of Ti₂AlNb-based alloys and the analysis of the coupling effects of strain rate, deformation temperature and strain on the deformation behavior of Ti₂AlNb-based alloys are necessary to study the thermal deformation law of Ti₂AlNb-based alloys and have important engineering significance for the preparation design and performance study of materials.

2. Materials

The Ti₂AlNb-based alloy was used for this experiment, and the chemical composition of this material is shown in table 1. This experimental material was compressed from a Φ8×12 mm cylinder on a Gleeble-3500 thermal simulation tester. The deformation temperature was 650-850°C with an interval of 50°C; the strain rate interval was 0.001-1s⁻¹; the maximum compression down was 40%, corresponding to a true strain of about 0.5, and the compression was water-cooled to room temperature immediately after completion.

Table 1. Chemical composition of Ti₂AlNb alloy(wt%).

Al	Nb	Mo	Fe	Si	Cu	Ni	Ti
10.6	41.2	0.88	0.047	0.07	<0.01	<0.01	Bal.

3. Results and Discussion

3.1. The Improved Z-A Model

The improved Z-A model was first proposed by Samantaray et al. [11] who, based on the Zerilli-Armstrong model, proposed a constitutive relationship between temperature and strain rate, and strain and flow stress, and the improved Z-A model can be expressed as:

$$\sigma = (a_1 + a_2 \varepsilon^m) \exp[-(a_3 + a_4 \varepsilon) T^* + (a_5 + a_6 T^*) \ln \dot{\varepsilon}^*] \quad (1)$$

where σ is the flow stress, MPa; ε is the strain; $\dot{\varepsilon}^* = \dot{\varepsilon} / \dot{\varepsilon}_r$ is the dimensionless strain rate, $\dot{\varepsilon}$ is the strain rate, s⁻¹, $\dot{\varepsilon}_r$ is the reference strain rate; $T^* = T - T_{ref}$, T is the thermodynamic

temperature, K, T_{ref} is the reference temperature, K; $a_1, a_2, a_3, a_4, a_5, a_6, m$ is the material constant. The reference temperature is the lowest deformation temperature, 923 K. The reference strain rate is set to $1s^{-1}$ and a_1 is the yield stress at the reference strain rate and reference deformation temperature, which is 19 MPa. At the reference strain rate, nine groups of strains with $\varepsilon=0.1-0.5$ at 923-1123K temperature, each spaced at 0.05, and the corresponding flow stress values are plotted for T^* versus $\ln\sigma$, as shown in figure 1. The values of $\ln(a_1 + a_2\varepsilon^m)$ and $-(a_3 + a_4\varepsilon)$ at strains 0.1 to 0.5 can be obtained from figure 1 as the intercept I_1 and slope S_1 , respectively, so that:

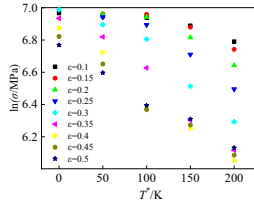


Figure 1. Relationship between $\ln\sigma$ and T^* at strain 0.1-0.5

$$I_1 = \ln(a_1 + a_2\varepsilon^m) \tag{2}$$

$$S_1 = -(a_3 + a_4\varepsilon) \tag{3}$$

Taking the natural logarithm of equation 2 again yields equation 4. After that $\ln a_2$ and m can be calculated from the fitted lines as the intercept and slope respectively, which are calculated as $a_2=852.1222$ and $m=-0.1477$.

$$\ln(\exp I_1 - a_1) = \ln a_2 + m \ln \varepsilon \tag{4}$$

The relationship between S_1 and ε can be obtained from equation 3. The intercept and slope of the fitted line are calculated for a_3 and a_4 respectively, $a_3=0.000532$, $a_4=0.00765$. Now take the natural logarithm of equation 1 to obtain equation 5.

$$\ln \sigma = \ln(a_1 + a_2\varepsilon^m) - (a_3 + a_4\varepsilon)T^* + (a_5 + a_6T^*)\ln \varepsilon^* \tag{5}$$

The relationship between $\ln\sigma$ and $\ln\varepsilon^*$ can be derived from equation 5, and the relationship is shown in figure 2, which allows the slope of the fitted line S_2 to be derived. The expression for S_2 is as follows:

$$S_2 = a_5 + a_6T^* \tag{6}$$

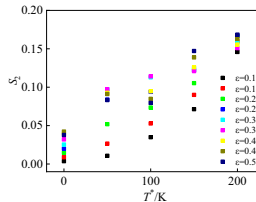


Figure 2. Relationship between S_2 and T^* at strain 0.1-0.5.

Finally the intercept and slope of the fitted line at strains 0.1-0.5 can be found from figure 2 as a_5 , a_6 respectively. The optimal a_5 and a_6 values were determined by comparing the minimised mean relative error E_{AR} , and it was concluded that the best E_{AR} was obtained for a_5 and a_6 at a strain of 0.2, 0.01092 and 0.0007147 respectively, and the corresponding E_{AR} value was also minimised to 12.4% with a correlation coefficient of 0.935. Finally, the a_1 , a_2 , a_3 , a_4 , a_5 , a_6 , m were substituted into the improved Z-A model to obtain the improved Z-A model for the Ti₂AlNb-based alloys as shown in equation 7, and the corresponding prediction results are shown in figure 3. It can be seen from figure 3 that the predicted flow stress values of the improved Z-A model are in poor agreement with the experimental values at strain rates of 0.001s⁻¹ and 1s⁻¹, which indicates that the improved Z-A model cannot predict the thermal deformation behaviour of the Ti₂AlNb-based alloys better.

$$\sigma = (19 + 852.1222\varepsilon^{-0.14771})\exp[-(0.000532 + 0.00765\varepsilon)T^* + (0.01092 + 0.0007147T^*)\ln\varepsilon^*] \quad (7)$$

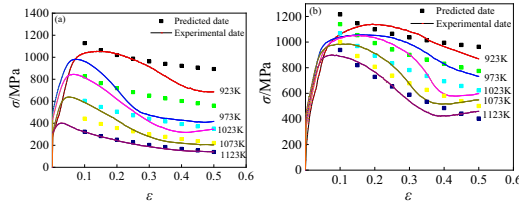


Figure 3. Comparison of predicted and experimental values for modified Z-A model at 0.001s⁻¹ and 1s⁻¹.

3.2. The Optimized Z-A Model

As mentioned previously, the improved Z-A model was unable to predict the thermal deformation behaviour of the Ti₂AlNb based alloys. In observing the above calculation process, it can be found that changes in strain affect the values of S_1 , I_1 , a_5 and a_6 , and the improved Z-A model does not take these changes into account, resulting in a lower prediction accuracy. In order to overcome these shortcomings, this paper uses polynomial functions to describe the relationship between S_1 , I_1 , a_5 , a_6 and strain in the range of strain 0.1-0.5, with 0.05 as the interval, and expresses the above parameters as a higher order polynomial function with strain, thus proposing an optimised Z-A model.

(1) Firstly the strain affects the I_1 value and the linear fit in the previous section does not describe the relationship between $\ln(\exp I_1 - a_1)$ and $\ln\varepsilon$ very well. After trying various orders a fifth-order polynomial fitting was chosen which better expresses the relationship between $\ln(\exp I_1 - a_1)$ and $\ln\varepsilon$, as shown in figure 4(a). Similarly a fifth-order polynomial fitting of $\exp I_1$ versus ε can be plotted and the relationship between $\exp I_1$ and ε is shown in figure 4(b). $\exp I_1$ can also be expressed as a fifth-order polynomial function on strain as shown in equation 8.

$$\exp I_1 = c_1 + c_2\varepsilon + c_3\varepsilon^2 + c_4\varepsilon^3 + c_5\varepsilon^4 + c_6\varepsilon^5 \quad (8)$$

The coefficients c_1 , c_2 , c_3 , c_4 , c_5 , c_6 of the fifth-order polynomial function in equation 8 are 1055.139, -865.109, 16585.81, -52561.7, 22713.2 and 39645.53 respectively.

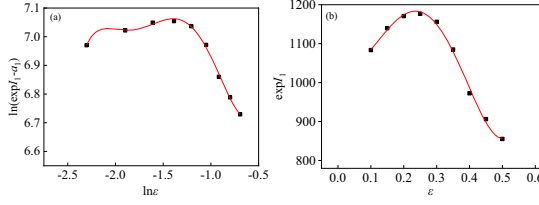


Figure 4. (a) Relationship between $\ln(\exp I_1 - a_1)$ and $\ln \varepsilon$; (b) Relationship between $\exp I_1$ and ε .

(2) Secondly the strain also affects the value of S_1 . The linear fit in the previous section was not able to express S_1 versus ε in a better way and now a fifth-order polynomial fitting is also used to express S_1 versus ε . The relationship is shown in figure 5 (a). Similarly, S_1 can be expressed as a fifth-order polynomial function with respect to strain, as shown in equation 9.

$$S_1 = j_1 + j_2 \varepsilon + j_3 \varepsilon^2 + j_4 \varepsilon^3 + j_5 \varepsilon^4 + j_6 \varepsilon^5 \quad (9)$$

(3) Finally the values of a_5 and a_6 also change due to changes in strain, so a_5 and a_6 are plotted against strain as shown in figures 5 (b) and (c) respectively, a_5 and a_6 are plotted as fifth-order polynomial functions with respect to strain as shown in equations 10 and 11.

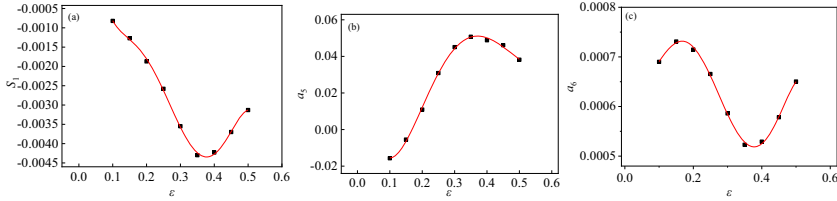


Figure 5. (a) Relationship between S_1 and ε ; (b) Relationship between a_5 and ε ; (c) Relationship between a_6 and ε .

$$a_5 = l_1 + l_2 \varepsilon + l_3 \varepsilon^2 + l_4 \varepsilon^3 + l_5 \varepsilon^4 + l_6 \varepsilon^5 \quad (10)$$

$$a_6 = p_1 + p_2 \varepsilon + p_3 \varepsilon^2 + p_4 \varepsilon^3 + p_5 \varepsilon^4 + p_6 \varepsilon^5 \quad (11)$$

Finally, by substituting equations 8, 9, 10 and 11 into the improved Z-A model, the optimized Ti₂AlNb-based alloys Z-A model can be obtained as shown in equation 12, and the prediction results of the optimized Ti₂AlNb-based alloys Z-A model are shown in figure 6.

$$\begin{cases} \sigma = \exp[I_1 + S_1 T^* + (a_5 + a_6 T^*) \ln \varepsilon^*] \\ I_1 = \ln(c_1 + c_2 \varepsilon + c_3 \varepsilon^2 + c_4 \varepsilon^3 + c_5 \varepsilon^4 + c_6 \varepsilon^5) \\ S_1 = j_1 + j_2 \varepsilon + j_3 \varepsilon^2 + j_4 \varepsilon^3 + j_5 \varepsilon^4 + j_6 \varepsilon^5 \\ a_5 = l_1 + l_2 \varepsilon + l_3 \varepsilon^2 + l_4 \varepsilon^3 + l_5 \varepsilon^4 + l_6 \varepsilon^5 \\ a_6 = p_1 + p_2 \varepsilon + p_3 \varepsilon^2 + p_4 \varepsilon^3 + p_5 \varepsilon^4 + p_6 \varepsilon^5 \end{cases} \quad (12)$$

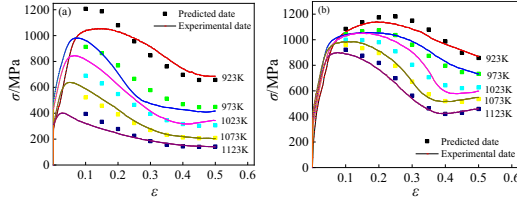


Figure 6. Comparison of predicted and experimental values for optimized Z-A model at $0.001s^{-1}$ and $1s^{-1}$.

3.3. Model Validation

As shown in figure 6, the optimised Z-A model can better predict the thermal deformation behaviour of the Ti_2AlNb -based alloy during the flow softening stage than the improved Z-A model, and the predicted flow stress values are in better agreement with the experimental values. In order to verify the accuracy of the model more accurately, statistical error analysis was performed using the mean relative error E_{AR} and correlation coefficient R as indicators to judge the accuracy of the model, which was further verified by the following expression:

$$E_{AR} = \frac{1}{N} \sum_{i=1}^N \left| \frac{E_i - P_i}{E_i} \right| \times 100\% \quad (13)$$

$$R = \frac{\sum_{i=1}^N (E_i - \bar{E})(P_i - \bar{P})}{\sqrt{\sum_{i=1}^N (E_i - \bar{E})^2} \sqrt{\sum_{i=1}^N (P_i - \bar{P})^2}} \quad (14)$$

In equations 13 and 14, E_i is the experimentally measured flow stress value, P_i is the flow stress value predicted by the Z-A model and N is the total amount of all data used. The correlation coefficient R is often used to indicate the linear correlation between the experimental and predicted values. The mean relative error, on the other hand, is an unbiased estimate for assessing the predictability of the constitutive model. The correlation between the predicted and experimental values of the optimised Z-A model is shown in figure 7, where the straight lines and dots indicate the best-fit and predicted flow stress values, and it can be seen that the data points are largely around the straight lines, and finally the R and E_{AR} values of the optimised Z-A model were calculated to be 0.964 and 10.5% respectively.

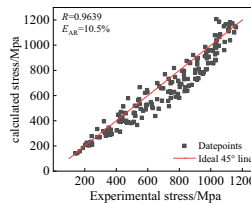


Figure 7. Optimized Z-A model correlation between predicted and experimental values.

Based on the above analysis it can be concluded that the optimised Z-A model can predict the thermal deformation behaviour of Ti_2AlNb based alloys better than the improved Z-A model, the predicted values are in better agreement with the experimental values, but the computational complexity is higher, the equations are

cumbersome and the calculations are larger. It is by taking the material parameters S_1 , I_1 , a_5 and a_6 into account that the flow stress values at each strain can be expressed in terms of multiple parameters, accuracy is guaranteed and the model is more widely used. If higher accuracy is required, the prediction accuracy can be improved by reducing the strain interval or adjusting the fitting order.

4. Conclusion

The improved Z-A model correlation coefficient R and the mean relative error E_{AR} were 0.935 and 12.4% respectively, while the optimized Z-A model correlation coefficient R and the mean relative error E_{AR} were 0.964 and 10.5% respectively. The improved Z-A model has simple equations but low fitting accuracy, while the optimized Z-A model can better predict the thermal deformation behaviour of Ti₂AlNb-based alloys with relatively high fitting accuracy.

Acknowledgement

This paper is supported by Natural Science Foundation of Jiangxi Province. The fund project number is 20202ACBL204001.

References

- [1] Li GQ, Ma FC, Liu P, et al. Review of micro-arc oxidation of titanium alloys: Mechanism, properties and applications. *Journal of Alloys and Compounds*. 2023; 948(5): 169773.
- [2] Liang ZQ, Xiao SL, Li QC, et al. Creep behavior and related phase precipitation of a creep-resistant Y2O₃-bearing high Nb containing TiAl alloy. *Materials Characterization*. 2023; 198: 112767.
- [3] Xue KM, Zhang YQ, Meng M, et al. Fracture behavior of B2 phase matrix of Ti₂AlNb-based alloy with microcracks of different orientations. *Engineering Fracture Mechanics*. 2023; 279: 109050.
- [4] Ju BY, Zhang NB, Deng TQ, et al. Anisotropic microstructure and mechanical properties of as-forged (Ti, Nb)B/Ti₂AlNb composites. *Materials Science and Engineering: A*. 2023; 24: 144935.
- [5] Li XW, Wang JH, Ma JX, et al. Thermal deformation behavior of Mg–3Sn–1Mn alloy based on constitutive relation model and artificial neural network. *Journal of Materials Research and Technology*. 2023; 24: 1802-1815.
- [6] Zerilli FJ, Armstrong RW. Dislocation - mechanics - based constitutive relations for material dynamics calculations. *Applied Physics*. 1987; 61: 1816-1822.
- [7] Samantary D, Mandal S, Bhaduri A. A comparative study on johnson cook, modified zerilli–armstrong and arrhenius-type constitutive models to predict elevated temperature flow behaviour in modified 9Cr–1Mo steel. *Computational Materials Science*. 2009; 47(2): 568-576.
- [8] Li TY, Zhao B, Liu XQ, et al. A comparative study on johnson cook, modified zerilli–armstrong, and arrhenius-type constitutive models to predict compression flow behavior of SnSbCu alloy. *Materials*. 2019; 12(10): 1726-1745.
- [9] Li F, Zhu CC, Li SJ, et al. A comparative study on modified and optimized Zerilli-Armstrong and arrhenius-type constitutive models to predict the hot deformation behavior in 30Si₂MnCrMoVE steel. *Journal of Materials Research and Technology*. 2022; 20: 3918-3929.
- [10] Sim KH, Ri YC, Jo CH, et al. Modified Zerilli-Armstrong and Khan-Huang-Liang constitutive models to predict hot deformation behavior in a powder metallurgy Ti-22Al-25Nb alloy. *Vacuum*. 2023; 210: 111749.
- [11] Samantary D, Mandal S, Borah U, et al. A thermo-viscoplastic constitutive model to predict elevated-temperature flow behaviour in a titanium-modified austenitic stainless steel. *Materials Science and Engineering: A*. 2009; 526(1-2): 1-6.